

## Effect of Rare Earth Oxide, Ho, on dc Electrical Degradation for Ni-MLCC

Hirokazu Chazono

Taiyo Yuden Co., Ltd., Central R&D Lab.  
5607-2 Nakamuroda Haruna-machi Gunma-gun Gunma 370-3347, Japan  
Fax: 81-27-360-8301, e-mail: hchazono@jty.yuden.co.jp

Effect of the amount of rare earth element, Ho, on electrical properties was investigated in dielectrics suitable for X5R-type Ni-MLCC. The amount of Ho,  $x$ , was changed from 0 to 2.0 in  $100\cdot\text{BaTiO}_3(\text{BT})-0.5\cdot\text{MgO}-x\cdot\text{HoO}_{3/2}$  system. The peak of the dielectric constant observed at around  $-40^\circ\text{C}$  for the sample without Ho was shifted as the amount of Ho increased up to 0.5 atom%. However, the lifetime under a highly accelerated life test for the samples with  $\leq 0.5$  atom% Ho was shorter compared with those for the samples with more than 0.8 atom% Ho. The nano-regional chemical composition analysis revealed that the Ho concentration in the shell phase was equivalent for samples containing 0.7 and 1.5 atom% Ho. However, Ho concentration in the grain boundary region was richer for the sample containing 1.5 atom% Ho than that for the sample containing 0.7 atom% Ho. The electrical conduction with various dc electrical fields at  $150^\circ\text{C}$  and the life-time under accelerated life test were considerably dependent on the amount of Ho. The role of Ho on the structure-property relationship was discussed.

Key words: rare earth, core-shell structure, electrical conduction, electrical degradation, accelerated life test

### 1. INTRODUCTION

Nowadays, the active layer thickness of multi-layer ceramic capacitors with Ni internal electrode (Ni-MLCCs) under mass-production is less than  $2\mu\text{m}$  to meet strong demands for larger capacitance and downsizing. The dielectrics must bear a considerably high electric field in such Ni-MLCCs with ultra-thin active layers. For instance, the electric field strength is as high as  $4\times 10^6\text{V/m}$  under the application of 6.3v dc to such Ni-MLCCs. Therefore, the improvement of the lifetime under simultaneously applied temperature and dc electrical field stresses has been the permanent challenge for MLCC suppliers. It is believed that the insulation resistance degradation of dielectric ceramics is caused by the oxygen vacancy electromigration toward the cathode, which was deduced by the experiments using thick sintered bodies and homogeneous systems. [1, 2]

However, it is well known that the temperature stable dielectrics suitable for X5R-type Ni-MLCC are composed of a heterogeneous microstructure, the so-called "core-shell" structure. [3, 4] Therefore, the model for dc electrical degradation presented in ref.1 should be modified to apply to the dielectrics in X5R-type Ni-MLCC due to the complicated microstructure and the too close distance between internal electrodes.

On the other hand, Okino *et al.* [5] showed that the lifetime at a highly accelerated life test (HALT) was considerably improved by adding the rare earth oxide having a small ionic radius, such as Dy, Ho, and Er. Today, the rare earth element, such as Dy, Ho and Y, is

preferably used as a key dopant for the dielectrics of Ni-MLCCs. These rare earth elements are known to be amphoteric through the investigation of the site occupancy in  $\text{BaTiO}_3$  (BT) lattice. [6, 7] However, the real role of the rare earth elements on the improvement of the lifetime at HALT has been still unclear.

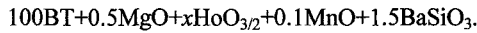
Measurement of the frequency response of the impedance is a powerful tool to investigate the correlation between the microstructure and electrical properties. [8] Recently, the author reported that 4-RC section electrical equivalent network determined by the frequency response of the impedance at elevated temperatures was successfully correlated to the microstructure, i.e., the core, shell, grain boundary (G.B.), and interface between dielectrics and internal electrodes, for X5R-type Ni-MLCC. [9] A new model on the dc electrical degradation in X5R-type Ni-MLCC was presented in ref.9. However, the role of doped rare earth element, Ho, was not fully understood in the previous study. Therefore, the aim of this study is to get a clue about the role of rare earth element, Ho, on the dc electrical degradation by investigating the effect of the amount of Ho on the microstructural development and electrical properties, especially on the conduction behavior.

### 2. EXPERIMENTAL

#### 2.1 Sample Preparation

The main starting material was BT with a nominal particle size of about  $0.35\mu\text{m}$  synthesized hydrothermally (Sakai Chemical Industry Co., Ltd.). Reagent grade MgO, MnO,  $\text{Ho}_2\text{O}_3$ , and  $\text{BaSiO}_3$  were

weighed and mixed to BT according to the composition described below.



In this study, the amount of Ho was changed from 0 to 2.0 atom%, i.e.,  $x = 0 \sim 2.0$ . They were mixed and then dried. These powders with an organic binder system were cast into green sheets. Ni internal electrode was formed on green sheets of about  $5\mu\text{m}$  by a conventional screen-printing. Twenty-one green sheets with Ni internal electrodes as well as the protective sheets at the upper and lower sides were stacked and pressed into a bar of about  $800\mu\text{m}$  thickness and then cut into small pieces. Terminal Ni electrodes were formed on both sides of the chips. The chips were fired at  $1280^\circ\text{C}$  and then cooled to  $1000^\circ\text{C}$  in a reducing atmosphere controlled by  $\text{H}_2$ ,  $\text{N}_2$ ,  $\text{O}_2$ , and  $\text{H}_2\text{O}$ , then to room temperature in a weakly oxidizing atmosphere ( $\text{P}_{\text{O}_2}=20\text{Pa}$  at  $1000^\circ\text{C}$ ).

## 2.2 Characterization

The MLCC samples were ground, ion-milled and then observed and analyzed in nano-regions by a high-resolution analytical electron microscope with an ultrathin-window energy dispersive X-ray detector (HR-AEM; TOPCON 002B, Akashi Co., Ltd., Japan). The sample and the milling stage were cooled with liquid nitrogen to avoid the creation of artifacts during the ion-milling treatment.

## 2.3 Electrical Properties

The temperature characteristics (TC) of the dielectric constant ( $\epsilon$ ) was measured at  $1\text{kHz}$ ,  $1.0\text{V}_{\text{rms}}$  using an LCR meter (HP-4284A; YHP, Japan), covering the temperature range from  $-55^\circ$  to  $140^\circ\text{C}$ . The dielectric constant of chip samples was calculated geometrically using the thickness and crossing area of the active layers. The current under various dc electrical fields at  $150^\circ\text{C}$  was measured until 180 sec using an ultra high resistance meter (R8340; Advantest, Japan). HALT was conducted at  $150^\circ\text{C}$  and  $18\text{V}/\mu\text{m}$ . The leakage current was monitored during the measurement.

## 3. RESULTS AND DISCUSSION

It is expected that TC is dependent on the amount of Ho when Ho amount in shell phase is dependent on the added Ho amount. Figure 1 shows the TC of  $\epsilon$  as a function of Ho amount for samples fired at  $1280^\circ\text{C}$ . There were two peaks at  $-40^\circ$  and  $125^\circ\text{C}$  for the sample with  $x = 0$ . The former peak was shifted towards a higher temperature as the Ho amount increased and then was constant at about  $50\sim 60^\circ\text{C}$  for samples with  $x > 0.5$ , while the latter peak was constant for all  $x$  values. The peak observed at around  $125^\circ\text{C}$  is the evidence that all the samples are composed of the core-shell structure. [3, 4]

In this system, Mg is incorporated into B-site in BT

perovskite lattice ( $\text{ABO}_3$ ) as an acceptor accompanied by the oxygen vacancy formation. It is known from our previous experiments that the incorporation of Mg occurred at a lower temperature than that of Ho determined by the precise X-ray diffraction analysis. Combining the results that Ho dissolved into A-site when the amount of Ho was small [6], it is supposed that the ratio of A- to B-site in BT lattice in the shell region is poor until  $x$  reaches to  $\sim 0.5$  since  $0.5\text{ atom}\%$  Mg occupies B-site before Ho fills A-site completely. The incorporation of Mg in the shell phase lowers the TC peak due to the oxygen vacancy formation. [10] Hence, the shift of the TC peak at around  $-40^\circ\text{C}$  to higher temperatures as the Ho amount increased can be ascribed to the incorporation of Ho into A-site accompanied by the decrease in the oxygen vacancy.

It is probable that the net A/B ratio has a close relationship between the rate of grain growth and the TC of  $\epsilon$ , especially at around the room temperature. No change in the peak of TC at around  $50\sim 60^\circ\text{C}$  for the samples with  $x > 0.5$  implies the saturation of Ho for A-site of BT lattice in the shell phase. The sample with  $x > 0.8$  showed the decrease in  $\epsilon$ . This can be ascribed to the severely inhibited grain growth due to too much existence of Ho in the G.B. [11] The chemical analysis in the shell region and G.B. must be necessary to elucidate the role of Ho on the grain growth behavior.

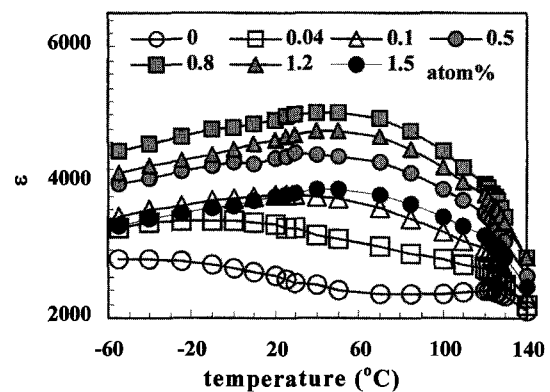


**Fig.1** TC of  $\epsilon$  as a function of Ho amount for the sample fired at  $1280^\circ\text{C}$ .

Figure 2 shows the micrographs observed by HR-AEM indicating the analytical points for the sample with  $0.7$  and  $1.5\text{ atom}\%$  Ho. Both samples showed a typical core-shell structure with well developed shell phase. Nano-regional composition at points indicated in Fig.2 were analyzed and plotted in Fig.3. The Ho concentration in the shell phase was identical and Ho did not exist in the center of core region irrespective of the initially added Ho amount. However, the Ho concentration in G.B. region was considerably dependent on the batch composition. It is noteworthy

that the Ho concentration in G.B. was smaller than that in the shell region when 0.7 atom% Ho was added while it was much greater in G.B. when 1.5 atom% Ho was added.

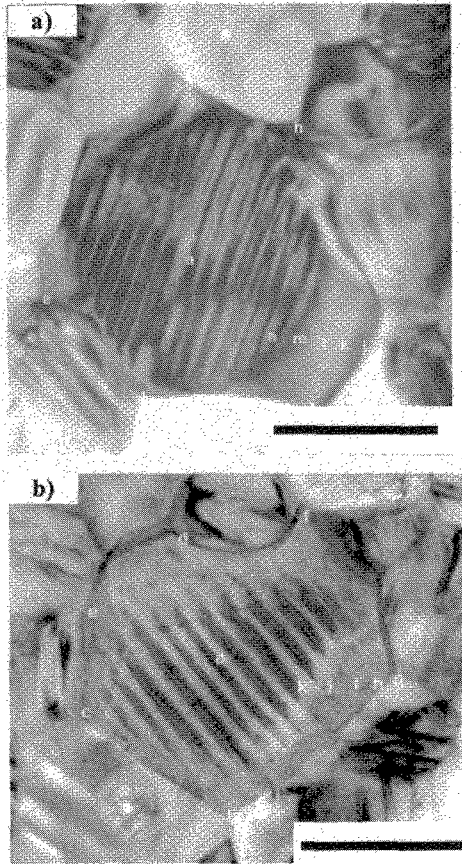


Fig.2 HR-AEM images for the sample with a) 0.7 and b) 1.5 atom%, indicating the analytical points. (bar=0.2 $\mu$ m)

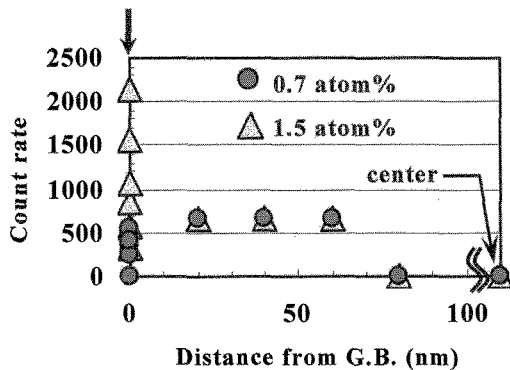


Fig.3 Intensity of Ho at various points indicated in Fig.3. Arrow indicates the position of G.B.

The Ho concentration in G.B. can affect the electrical conduction behavior. Therefore, the time dependence of the leakage current at various dc electrical fields (I-t) was measured next. Figure 4 shows the I-t characteristics for the sample with  $x = 0.2$  measured at 150°C. The leakage current was monitored for 180s. The leakage current decreased as the time passed when the electrical field was low ( $\leq 5$  V/ $\mu$ m). However, the leakage current increased when the electrical field was high ( $\geq 12$  V/ $\mu$ m).

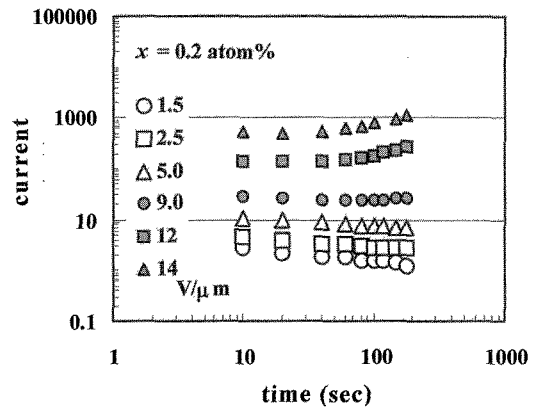


Fig.4 I-t characteristics at 150°C and various dc electrical field for the sample fired at 1280°C with  $x = 0.2$ .

Using the result of I-t characteristics measured at 150°C, the leakage current was plotted against applying dc voltages (I-V characteristics) in Fig.5. All the plots in Fig.5 are taken from the leakage current at 180 sec in I-t measurement and the filled symbols indicate the current which increased during the I-t measurement indicating the degraded insulation resistance. It was found that a higher dc voltage could be applied and a higher current conducted through the sample as the Ho amount

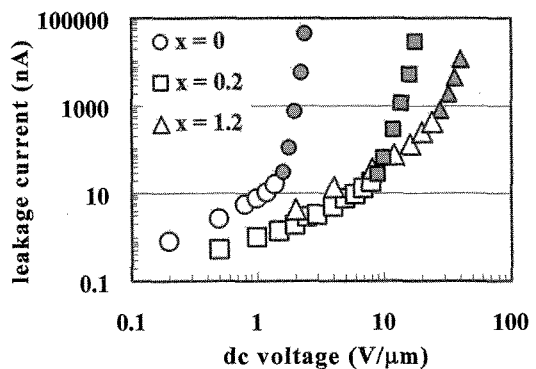


Fig.5 I-V characteristics at 150°C for samples fired at 1280°C with  $x = 0, 0.2,$  and  $1.2$  atom%, where filled symbols denotes the gradually increasing current during I-t measurement.

increased. For example, the leakage current, as high as  $0.5\mu\text{A}$  ( $\sim 0.05\text{A}/\text{m}^2$ ), conducted stably through the sample containing 1.2 atom% Ho at  $24\text{V}/\mu\text{m}$ . Moreover, the I-V characteristics was nonlinear especially for the sample with  $x = 1.2$  in which the nonlinearity coefficient was 1.8. On the contrary, the maximum leakage current (open symbol) was almost the same for samples with 0 and 0.2 atom% Ho, although the higher dc voltage could be applied as the Ho content was increased. The increase in applicable dc voltage without degradation can be ascribed to the increase in the resistivity of shell region due to the incorporation of Ho into shell phase. The fact that the maximum leakage current was almost identical for samples with  $x = 0$  and 0.2 implies that G.B. characteristics for both samples were almost identical. Therefore, the G.B. characteristics for the sample with  $x = 1.2$  is considerably different from those for sample with  $x = 0$  and 0.2.

It is interesting to investigate the effect of Ho amount on the lifetime at HALT. The characterized lifetime after Waser *et al.* [1] at HALT under the condition of  $150^\circ\text{C}$  and  $18\text{V}/\mu\text{m}$  is shown in Fig.6 for the sample fired at  $1280^\circ\text{C}$  as a function of  $x$  values. As expected from the I-V characteristics seen in Fig.5, the characterized lifetime for the sample without Ho was zero. The characterized lifetime was also zero for samples with  $x = 0.04$  and 0.1. However, the characterized lifetime was considerably improved as the Ho amount increased.

The larger mean grain size indicates the thicker shell since all the sample is composed of core-shell structure judged from the observation of the TC peak at around  $125^\circ\text{C}$  in Fig.1. The thicker shell can bring about a longer lifetime at HALT. [12] This must be one of the cause of the longer lifetime at HALT for the samples with  $x \geq 0.2$  in Fig.6. However, the sample could conduct a higher conduction current as the Ho amount was increased. This finding is not simply implying that the life is improved by the thicker shell since the thicker shell brought about the lower leakage current during HALT seen in ref.12.

On the other hand, the author proposed the tunneling current conducting through the G.B. in a similar system having the nonlinearity coefficient of 1.65 at  $240^\circ\text{C}$ . [9] The nonlinearity of I-V characteristics observed in the sample with  $x = 1.2$  implies the occurrence of the tunneling conduction. This nonlinear I-V characteristics was not observed in samples with  $x = 0$  and 0.2 since the insulation resistance was degraded at low applying dc voltages for both samples. This change in conduction mechanism for the sample with 1.2 atom% Ho can be caused by the existence of Ho rich in the G.B. region as seen in Fig.3.

The concentration of Ho in G.B. region must be fatal for the electrical degradation. Even with  $x = 0.04$  and 0.1, TCC was changed although the characterized lifetime

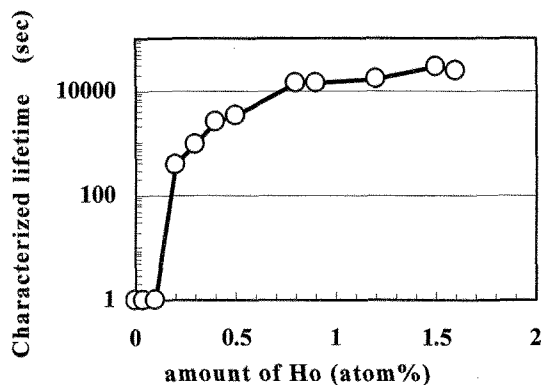


Fig.6 Characterized lifetime at  $150^\circ\text{C}$  and  $18\text{V}/\mu\text{m}$  as a function of Ho amount.

was not improved at all. The peak of  $\epsilon$  around room temperature continued to shift toward higher temperature until  $x = 0.5$  although the characterized lifetime was shorter compared with the sample with  $x > 0.8$ . This finding suggests that the solubility of Ho in the shell phase is less than 0.5 atom% of batch Ho composition. The author reported that the core/shell volume ratio was nearly 5/5 in ref.9. Therefore, it is assumed that the saturated concentration of Ho in the shell phase should be less than 1 atom%. Kishi *et al.* reported in ref.6 that the secondary phase,  $\text{R}_2\text{Ti}_2\text{O}_7$ , was observed in the sample with 2 atom% Ho and 1 atom% Mg but it was not observed in the sample with 1 atom% Ho and 0.5 atom% Mg in the model system of  $(\text{Ba}_{1-2x}\text{Ho}_{2x})(\text{Ti}_{1-x}\text{Mg}_x)\text{O}_3$  solid solution. Therefore, it can be concluded that the obtained saturated concentration of Ho in the shell phase in this study is almost consistent with that reported by Kishi *et al.*

The incorporation of Ho into A-site when the added Ho amount is small can improve the resistivity of the shell phase since the oxygen vacancy is eliminated by incorporating Ho in shell phase as a donor. This brings about the increase in  $\epsilon$ , especially around room temperature and increase in the applicable dc bias without degradation. However, the conducting current was about 20 nA more or less and the characterized lifetime was short. The considerable improvement of the characterized lifetime was brought about by adding Ho more than 0.8 atom% accompanied by the increase in the conduction current.

It should be noted that the higher current does not mean the lower lifetime as long as the electric carrier is responsible for the conduction. Therefore, it is concluded that the high concentration of Ho in G.B. region brings about the change in conduction mechanism. This can be caused by introducing the tunneling conduction through the back-to-back Schottky barrier at G.B. However, the great improvement of characterized lifetime can be caused by the rich existence of Ho in G.B. region which is effective to

inhibit the electromigration of positively charged oxygen vacancies since G.B. will be positively charged by  $\text{Ho}^{3+}$ .

Figure 7 shows the impedance plane measured at 280°C for samples with  $x=0.5, 1.0, 1.2,$  and  $1.5$ . It was found that the equivalent electrical network for samples with  $x=1.2$  and  $1.5$  was 4-RC while that for the sample with  $x=0.5$  was 5-RC. From Fig.7, it is clearly understood that the 5th RC component is observed at the lowest frequency region for the sample with  $x=0.5$  implying the dipole of slow motion. However, the 5th RC component was eliminated as the Ho amount increased. It is possible that the 5th RC component is originated from the migration of oxygen vacancy across the G.B. due to almost no precipitation of  $\text{Ho}^{3+}$  in G.B. region.

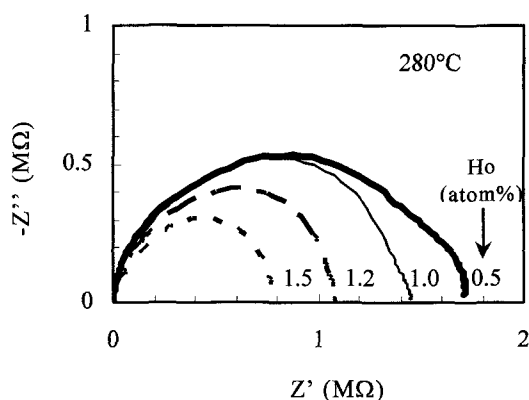


**Fig.7 Complex impedance plane, so-called “Cole-Cole’s plot,” measured at 280°C for samples having various Ho amounts.**

Further investigation of the physical and chemical states for Ho existing in G.B. region must be necessary to clearly understand the precise roles of Ho for the improvement of characterized lifetime.

#### 4. CONCLUSION

Effect of the amount of Ho on electrical properties was investigated in dielectrics suitable for X5R-type Ni-MLCC. The amount of Ho,  $x$ , was changed from 0 to 2.0 in  $100\cdot\text{BaTiO}_3(\text{BT})\cdot 0.5\cdot\text{MgO}\cdot x\cdot\text{HoO}_{3/2}$  system.

The nano-regional chemical compositional analysis revealed that the saturated Ho concentration in the shell phase was less than 1 atom%. Moreover, Ho concentration in G.B. region was richer than that in the shell phase when the Ho amount was 1.5 atom% while it was richer in the shell phase when the Ho amount was 0.7 atom%.

The peak of the dielectric constant observed at around  $-40^\circ\text{C}$  for the sample without Ho was shifted as the amount of Ho increased up to 0.5 atom%. I-V characteristic measurement revealed that a higher dc voltage could be applied and a higher current could

conduct through the sample as the Ho amount was increased. The lifetime under a highly accelerated life test (HALT) was zero for the sample with  $x=0, 0.04,$  and  $0.1$ . The lifetime was improved as the Ho amount was increased to 0.5 atom%. However, it was shorter compared with those for the sample with more than 0.8 atom% Ho. It was found that Ho was incorporated into A-site in BT perovskite lattice first, and then Ho preferred to exist in G.B. region when the Ho amount was increased more than 0.7 atom%. High concentration of Ho in G.B. region changed the conduction mechanism resulted in considerably improved lifetime at HALT.

#### 5. REFERENCES

- [1] R. Waser, T. Baiatu, and K. -H. Härdtl, *J. Am. Ceram. Soc.*, **73** (1990), p.1645.
- [2] J. Sheng, T. Fukami, and J. Karasawa, *J. Electrochem. Soc.*, **145** (1998), p.1592.
- [3] H. Chazono and H. Kishi, *J. Am. Ceram. Soc.*, **83** (2000), p.101.
- [4] H. Chazono and H. Kishi, CSJ Series –Publications of the Ceramic Society of Japan, Vol.8, *Electroceraamics in Japan IV*, Edited by, M. Murata, T. Kimura, S. Fujitsu, and K. Shinozaki, (Trans Tech Publications Ltd., Switzerland, 2002), p.47.
- [5] Y. Okino, H. Shizuno, S. Kusumi, and H. Kishi, *Jpn. J. Appl. Phys.*, **33** (1991), p.5393.
- [6] H. Kishi, N. Kohzu, J. Sugino, H. Ohsato, Y. Iguchi, and T. Okuda, *J. Europ. Ceram. Soc.*, **19** (1999), p.1043.
- [7] Y. Tsur, A. Hitomi, I. Scrymgeour, and C. A. Randall, *Jpn. J. Appl. Phys.*, **40** (2001), p.255.
- [8] M. Vollmann and R. Waser, *J. Am. Ceram. Soc.*, **77** (1994), p.235.
- [9] H. Chazono and H. Kishi, *Jpn. J. Appl. Phys.*, **40** (2001), p.5624.
- [10] K. H. Härdtl and R. Wernicke, *Solid State Commun.*, **10** (1972), p.153.
- [11] H. Chazono, T. Hagiwara, H. Kishi, Proc. 11<sup>th</sup> US-Jpn. Seminar on Dielectric and Piezoelectric Ceramics, Sapporo, Japan, (2003) 1-5.
- [12] Y. Mizuno, T. Hagiwara, H. Chazono, and H. Kishi, *J. Europ. Ceram. Soc.*, **21** (2001), p.1649.

(Received October 11, 2003; Accepted March 10, 2004)